

film drained but the flows were confined between fixed walls, and so the drainage was slow.

Our polymer films were "bare": There were no surfactants added and no pollution (such as proteins on water films or dust particles). The trick was to use a liquid of very low surface tension (such as silicones or fluorinated chains): Pollutants do not adsorb easily on these surfaces.

A final remark on the death of our films: The detailed viscoelastic properties of our materials did not show up in our systems. However, the existence of a high-frequency regime where the material behaves like an elastic solid (of shear modulus μ) is crucial. It enables the propagation of the Laplace stress up to a distance $2cT_r$. One common and essential feature of our systems is that cT_r was larger than the sample size.

The present experiments focused on two model systems: linear polymer melts

and conventional glasses. However, our findings may be transposed to other viscoelastic systems, for instance, physical gels with no permanent cross-links and possibly the cytoskeletons, such as the spectrin network of red blood cells and other biological gels (9).

REFERENCES AND NOTES

1. For a review, see J. Lucassen, in *Anionic Surfactants* (Dekker, New York, 1981).
2. K. Mysels, K. Shinoda, S. Frenkel, *Soap Films* (Pergamon, London, 1959); D. Weaire, N. Pittet, S. Hutzler, *Phys. Rev. Lett.* **71**, 2670 (1993); E. Ruckenstein and A. Bhakta, *Langmuir* **11**, 1486 (1995).
3. For a review, see P.-G. de Gennes, *Faraday Discuss.* **104**, 1 (1996).
4. M. T. Mangau and K. V. Cashman, *J. Volcanol. Geotherm. Res.* **73**, 1 (1996).
5. G. Debregas, P. Martin, F. Brochard-Wyart, *Phys. Rev. Lett.* **75**, 3886 (1995).
6. See, for instance, L. D. Landau and E. M. Lifshits, *Theory of Elasticity* (Pergamon, London, 1959), chap. 25, p. 110. The velocity $2c$ is expected when the Lamé coefficients λ and μ satisfy $\mu \ll \lambda$.
7. The time required for the slide to reach its final temperature cannot be easily determined. However, we noted that the visible onset of the hole opening was systematically of order 200 s. By limiting our observations to relatively low temperatures ($T < 812^\circ\text{C}$), we could decouple this delay and the characteristic time for hole opening (on the order of 15 min to 2 hours). The rapid decrease of the viscosity with decreasing temperature makes the onset of the growth process sharp (Fig. 3A) and indicates that the whole measurement is done at a constant temperature. The biggest uncertainty comes from fluctuations in the oven temperature, which are of the order of $\pm 0.5^\circ\text{C}$.
8. P.-G. de Gennes, *C. R. Acad. Sci. Ser. II* **305**, 9 (1987).
9. M. Lindemann, M. Steinmetz, M. Winterhalter, *Prog. Colloid Polym. Sci.* **105**, 209 (1997).
10. R. H. Doremus, *Glass Science* (Wiley, New York, ed. 2, 1995), chap. 11.
11. Bursting experiments on viscous bubbles were performed at Rhône-Poulenc Research (St. Fons, France). We thank L. Vovelle and J. J. Martin for their help. We would like to acknowledge the support of H. Arribart and S. Creux, from the CNRS–St. Gobain research laboratory (Aubervilliers, France), where the experiments on glass slides were done. We are grateful to A. Buguin, R. Fondecave, and P. Martin for fruitful comments on this work.

20 October 1997; accepted 2 February 1998

Deuterium in Comet C/1995 O1 (Hale-Bopp): Detection of DCN

Roland Meier,*† Tobias C. Owen,* David C. Jewitt,*
Henry E. Matthews, Matthew Senay,* Nicolas Biver,
Dominique Bockelée-Morvan, Jacques Crovisier, Daniel Gautier

Deuterated hydrogen cyanide (DCN) was detected in a comet, C/1995 O1 (Hale-Bopp), with the use of the James Clerk Maxwell Telescope on Mauna Kea, Hawaii. The inferred deuterium/hydrogen (D/H) ratio in hydrogen cyanide (HCN) is $(D/H)_{\text{HCN}} = (2.3 \pm 0.4) \times 10^{-3}$. This ratio is higher than the D/H ratio found in cometary water and supports the interstellar origin of cometary ices. The observed values of D/H in water and HCN imply a kinetic temperature $\geq 30 \pm 10$ K in the fragment of interstellar cloud that formed the solar system.

We detected deuterated water (HDO) in Comet C/1995 O1 (Hale-Bopp) (1). This detection resulted in the third measurement of the D/H ratio in cometary water, which appears to be essentially the same in Comets P/Halley, C/1996 B2 (Hyakutake), and

Hale-Bopp, $D/H = (3.16 \pm 0.34) \times 10^{-4}$ (2). If comets have preserved unmodified interstellar material, we expect hydrogen-containing compounds other than H_2O to exhibit different values of D/H, a well-known result of ion-molecule reactions in interstellar clouds (3). We made several attempts to detect DCN in Hale-Bopp, to test this prediction, because HCN exhibits the most prominent emission lines of any hydrogenated species detected in cometary millimeter and submillimeter spectra thus far. Our initial effort was made before perihelion and did not succeed. Here, we report our detection of DCN from observations of Hale-Bopp using the James Clerk Maxwell Telescope (JCMT) on Mauna Kea, Hawaii,* near the comet's peak activity and under more favorable atmospheric conditions.

The $J = 5-4$ rotational transition of DCN at 362.0465 GHz was detected on a

spectrum (Fig. 1) recorded on 28.0 April 1997 (UT). At the time of these observations, Hale-Bopp was about 1 month past perihelion at a heliocentric distance of 1.031 astronomical units (AU) and 1.72 AU distant from Earth.

We obtained the observations with the JCMT using a dual-channel heterodyne receiver ("B3") sensitive to submillimeter radiation, with subsequent signal processing effected with an autocorrelation spectrometer. Sky background emission was removed by frequency switching ± 8.1 MHz once every 30 s. Receiver B3 uses two low-noise niobium junctions that simultaneously detect orthogonally polarized radiation from the same point on the sky. Radiation incident on B3 is detected in two sidebands separated by 8.0 GHz. By means of a dual-beam interferometer in the beam path within the receiver, the "image" sideband was almost entirely suppressed, and the "signal" sideband was transmitted and the temperature scale well established. We tuned the receiver such that the DCN 5-4 line, arising in the signal sideband, appeared in the spectrum displaced from HCN 4-3, which, at a frequency of 354.5055 GHz, arose in the image sideband. Although the HCN 4-3 line was suppressed by a factor of about 25 by the image sideband rejection, the emission from it allowed us to monitor the quality of the telescope pointing very effectively.

Hale-Bopp was a daytime object during these observations with a solar elongation of only 33° . JCMT is protected by a Gore-Tex wind blind from direct solar radiation, which limits the deformation of the telescope surface due to heating. Pointing and

R. Meier, T. C. Owen, D. C. Jewitt, N. Biver, University of Hawaii, Institute for Astronomy, 2680 Woodlawn Drive, Honolulu, HI 96822, USA.

H. E. Matthews, National Research Council of Canada, Herzberg Institute of Astrophysics, 5071 West Saanich Road, Victoria, BC V8X 4M6, Canada, and Joint Astronomy Centre, 660 North A'Ohoku Place, Hilo, HI 96720, USA.

M. Senay, Five College Radio Astronomy Observatory, University of Massachusetts, Amherst, MA 01003-4517, USA.

D. Bockelée-Morvan, J. Crovisier, D. Gautier, Observatoire de Paris-Meudon, 5 Place Jules Janssen, F-92195 Meudon, Cedex, France.

*Visiting astronomer at the James Clerk Maxwell Telescope, 600 North A'Ohoku Place, Hilo, HI 96720, USA.

†To whom correspondence should be addressed: E-mail: meier@uhifa.ifa.hawaii.edu

focus offsets were monitored with nearby sources of strong continuum emission. The observed offsets did not exceed 3.5 arc sec. At 362 GHz, the full width at half maximum (FWHM) of the main beam was 12.5 ± 0.4 arc sec. Also, before the start of the DCN observations, we verified the ephemeris of Hale-Bopp by taking an image of the comet coma at $850 \mu\text{m}$ with the bolometer camera SCUBA (4).

All bright lines of HCN suffer from opacity effects. These problems can be avoided if corresponding lines in the rare isotopic species H^{13}CN are used and if the

$^{13}\text{C}/^{12}\text{C}$ ratio in HCN is known. The 5–4 transition of H^{13}CN at 431.660 GHz, the counterpart to DCN 5–4, is inaccessible to JCMT, and we used the next lowest transition, H^{13}CN 4–3 at 345.340 GHz. The HCN 4–3 line is a composite of six hyperfine components, of which $F(3-3)$ and $F(4-4)$ (5) are resolved as extended winglets to the main line. Each of the two components carries 2.08% of the total line flux. These winglets can be used to determine the optical depth of the HCN (4–3) line independent of the H^{13}CN line (6, 7). To derive a $(\text{D}/\text{H})_{\text{HCN}}$ ratio in HCN, no

absolute calibration was necessary because we are only interested in ratios of lines that were obtained with the same antenna and the same receiver at about the same frequencies. Nevertheless, we still needed to use a model and make a few assumptions. First, we assumed a solar system ratio of 89.9 for $^{12}\text{C}/^{13}\text{C}$ in HCN (8) in agreement with a recent study of H^{13}CN , HC^{15}N , and C^{34}S in Hale-Bopp (7). Second, we assumed that the hyperfine components $F(3-3)$ and $F(4-4)$ and the lines of H^{13}CN and DCN were optically thin. At the time of our observations, the total line strength of HCN was reduced by about 30% because of optical depth. This reduction indicates modest optical depth in HCN and implies that the faint hyperfine components $F(3-3)$ and $F(4-4)$ are optically thin. The fact that the rare isotopomers of HCN are about two or three orders of magnitude less abundant than HCN suggests that H^{13}CN and DCN are also optically thin. Third, we used two different models to assess the relative line strengths of HCN and its isotopes (Table 1). Our main beam probed the innermost ± 8000 km of the coma where the high gas density resulted in a distribution of the level population controlled largely by collisions. Therefore, our first model, which assumed thermal equilibrium at a uniform rotational temperature of 90 K (9) (Table 1, τ_1), was already very accurate. It turned out that any rotational temperature between 70 and 120 K yields the same line ratio for the relevant lines within a few percent. Our second model was more detailed and closely followed a concept of Crovisier (10). This time, fluorescence excitation of the strongest parallel and perpendicular infrared (IR) bands was included. We adopted a temperature profile that mimics expansion cooling and photolytic heating at a beam-averaged rotational temperature of ~ 90 K. This second model confirmed that fluorescence did not substantially affect relative line strengths (Table 1, τ_2).

The complete (DCN, H^{13}CN , and HCN) data set was obtained in two observing shifts of 8 hours each. On the day before the DCN observations and over the course of several months, we measured the $\text{H}^{13}\text{CN}/\text{HCN}$ ratio as a function of the HCN line intensity. During the DCN exposure, we obtained observations of HCN. We chose to observe HCN rather than H^{13}CN for a reference because the rare isotopomer would have required a mechanical retuning of the receiver and a much longer integration time. The HCN observations were then converted to H^{13}CN brightnesses with the appropriate $\text{H}^{13}\text{CN}/\text{HCN}$ ratio from the previous day. If we ratio the DCN line with the H^{13}CN line and apply the relative line strengths (Table

Fig. 1. The J 5–4 line of DCN in Comet C/1995 O1 (Hale-Bopp). The dotted line shows scaled HCN 4–3, the residual line obtained in the “image” sideband, overlaid on the same velocity scale as DCN 5–4 (solid line). Data were obtained in a single sideband mode at a spectral resolution of $\Delta\nu = 0.1562$ MHz. The displayed spectrum is a composite of 19 10-min exposures and 1 2-min exposure (= 11,520 s total exposure time). Frequency switching causes two ghost lines that are visible at around ± 14 km s^{-1} .

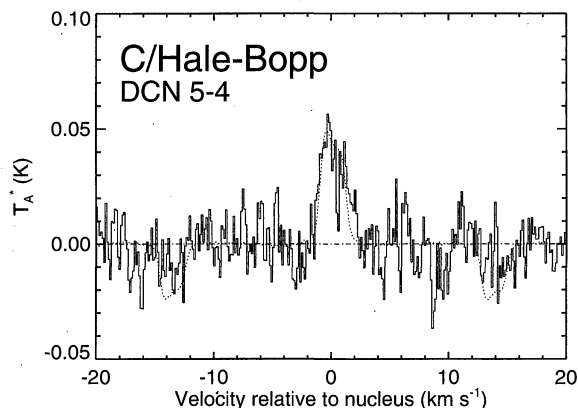


Fig. 2. The D/H ratio in H_2O (solid lines) and HCN (dashed lines). The curves show calculated D/H ratios as a function of the temperature in dense interstellar clouds that have reached thermal equilibrium ($t \approx 10^8$ years) and are dominated by gas-phase chemistry [after (17)]. The calculations use dissociative recombination branching ratios that are based on the idea that the breaking of bonds between heavy atoms is less favored compared with the ejection of single and multiple hydrogen atoms (37). We do not show “early-time” models ($t \approx 10^5$ years) because they lead to results inconsistent with the measured D/H ratio in cometary H_2O . Horizontal lines show the measured cometary D/H ratio in H_2O (solid line) and HCN (dashed line). For H_2O , we used the value by Meier *et al.* (1), whereas for HCN we used the result derived in this paper. Dotted areas indicate 1σ errors.

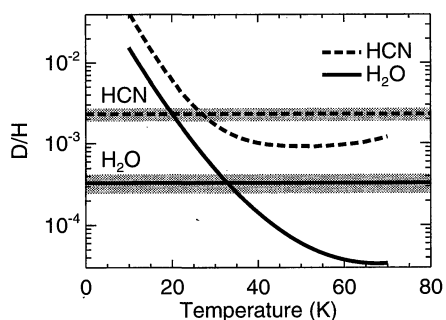


Table 1. Parameters relevant to the D/H ratio in HCN. Line frequencies ν are from (29). $\int T_A d\nu$ is the line-integrated antenna temperature. One day before the DCN observation, we measured $[\text{HCN } 4-3/\text{H}^{13}\text{CN } 4-3] = 70.3 \pm 6.2$. This ratio and the antenna temperature of the HCN 4–3 line during the DCN exposure (see below) were used to calculate the H^{13}CN line intensity. Ratio $r_i = [X/\text{DCN } 5-4]$, with $i = 1$ or 2 and X referring to the molecular transition listed in the first column of this table, is defined as the relative line intensity between transition X and the 5–4 transition of DCN if we assume equal abundances for all isotopomers of HCN. Ratio r_1 was evaluated at a constant rotational temperature of 90 K with the assumption of thermal equilibrium. Ratio r_2 is based on a model that includes fluorescence pumping of the strongest IR bands and a more realistic temperature profile with a beam-averaged rotational temperature of ~ 90 K. For HCN, we adopted the “ g factors” of the perpendicular (g_{\perp}) and two parallel (g_{\parallel}) IR bands from (10). The g factors for H^{13}CN are guesses. The DCN values were derived from spectroscopic laboratory data by Kim and King (30).

Transition X	ν (GHz)	$\int T_A d\nu$ (K km^{-1} s^{-1})	r_1	r_2	g_{\perp} (s^{-1})	g_{\parallel} (s^{-1}) \cdot
DCN 5–4	362.0464842	0.103 ± 0.010	1.00	1.00	1.6×10^{-5}	1.5×10^{-4}
H^{13}CN 4–3	345.3397599	0.528 ± 0.047	1.02	1.05	6.2×10^{-5}	3.3×10^{-4}
HCN 4–3	354.5054759	37.1 ± 0.7	1.07	1.10	7.9×10^{-5}	3.7×10^{-4}

1), we derive a D/H ratio in HCN of $(D/H)_{\text{HCN}} = (2.3 \pm 0.4) \times 10^{-3}$. The uncertainty of the D/H ratio is a 1σ error that includes statistical errors of all measured quantities and a 10% model uncertainty in the ratio r_i . If we use the hyperfine lines instead, we obtain a D/H ratio $(D/H)_{\text{HCN}} = (2.3 \pm 0.5) \times 10^{-3}$. The two methods yield the same result, and we will use $(D/H)_{\text{HCN}} = (2.3 \pm 0.4) \times 10^{-3}$ in the following discussion (11, 12).

The fact that D/H in Hale-Bopp's HCN is about seven to eight times the ratio in cometary H_2O provides evidence in favor of the interstellar origin of cometary ices. The HCN and H_2O in this comet had no opportunity to exchange D with the much more abundant H_2 in the nebula. In the H_2 , D/H was about 2×10^{-5} to 4×10^{-5} (13), so that such an exchange would have lowered the values of D/H in H_2O and HCN and brought them into closer agreement with each other. We can therefore conclude, for example, that H_2O from the inner nebula near the sun, whose D/H could have been lowered to less than 10^{-4} in this way (14), was not carried out to participate in the formation of these comets. We can also conclude that comets were not formed in the subnebulae of giant planets, as proposed by Fegley and Prinn (15), for the same reason.

However, it is common to find differing values of D/H among different molecular species in a given interstellar cloud (16, 17). For ion-molecule reactions, the amount of D enrichment compared with D/H in H_2 is strongly dependent on temperature (Fig. 2). Gas-grain surface reactions in such clouds could produce similar enrichments to those illustrated in Fig. 2 at higher temperatures (18). Unfortunately, they are more difficult to predict quantitatively. What seems clear, however, is that the temperature in the cloud fragment from which the solar system formed could not have been colder than 30 ± 10 K (Fig. 2).

This temperature is considerably higher than the cloud temperature of ~ 10 to 15 K assumed in some models for making comets from interstellar grains (19), with consequences for the abundances and state of the molecules expected to be present in comet nuclei. These temperatures overlap with the range associated with the Uranus-Neptune region of the solar nebula (50 ± 20 K) (20), the commonly accepted source region of the majority of comets now in the Oort cloud. Thus, even if the icy mantles on interstellar grains sublime as the grains fall toward the midplane of the outer solar nebula (21), recondensation will occur at about the same temperature at which the ice originally formed (22). One consequence of this coincidence will be the absence of neon in

cometary ice, even if that ice never experienced sublimation and recondensation during the formation of the nebula. Unlike argon, krypton, and xenon, neon atoms are sufficiently small that they could not be trapped in ice unless the ambient temperature is below 20 K (23). The recent upper limit of $\text{Ne}/\text{O} \leq 0.005$ solar set by Krasnopolsky *et al.* (24) is consistent with this prediction, as is the absence of detectable amounts of Ne on Titan, Triton, and Pluto, three icy bodies with nitrogen-dominated atmospheres. It appears that the Ne now found in the atmospheres of the inner planets must therefore have a noncometary source, as previously suggested (23).

Another implication is that cometary ices will have to be diluted with some hydrogen reservoir having a low D/H ratio, in order to match Earth's oceans (1, 2) or to achieve the values of D/H found in the atmospheres of Uranus and Neptune (25). On the basis of observations of molecules in interstellar clouds, even higher D/H enrichments than in HCN can be expected in many hydrocarbons, such as C_3H_2 , C_2H_n , or H_2CO , with D/H ratios as high as 1% (26). Under solar ultraviolet irradiation, many of these hydrocarbons produce CH radicals, which fluoresce at ~ 4305 Å ($A^2\Delta - X^2\Pi$ band system). A recent study of Hyakutake demonstrated that for a bright comet current, ground-based, high-resolution spectrometers could be able to detect CD down to the 1% level (27).

REFERENCES AND NOTES

1. R. Meier *et al.*, *Science* **279**, 842 (1998).
2. Halley: P. Eberhardt, M. Reber, D. Krankowsky, R. R. Hodges, *Astron. Astrophys.* **302**, 301 (1995); H. Balsiger, K. Altwegg, J. Geiss, *J. Geophys. Res.* **100**, 5287 (1995). Hyakutake: D. Bockelée-Morvan *et al.*, *Icarus*, in press. As explained in (1), the quoted value is the in situ determination in Halley, which has a much higher precision than remote measurements.
3. This theory was developed by W. D. Watson [*Rev. Mod. Phys.* **48**, 513 (1976)]. Observations have been summarized, for example, by W. M. Irvine and R. F. Knacke (26) and E. F. van Dishoeck, G. A. Blake, B. T. Draine, and J. I. Lunine [in *Protostars and Planets III*, E. H. Levy and J. I. Lunine, Eds. (Univ. of Arizona Press, Tucson, 1993), pp. 163–241].
4. The Submillimetre Common-User Bolometer Array (SCUBA) for JCMT. SCUBA can also observe at 450 μm with an array of 91 bolometers.
5. F is the quantum number for the total angular momentum including nuclear spin. The nuclear quadrupole moment of the ^{14}N atom in HCN and DCN leads to a hyperfine splitting of the lower rotational levels J [Nguyen-Van-Than and I. Rossi, *J. Mol. Spectrosc.* **157**, 68 (1993)].
6. D. Bockelée-Morvan, R. Padman, J. K. Davis, J. Crovisier, *Planet. Space Sci.* **42**, 655 (1994).
7. D. C. Jewitt, H. E. Matthews, T. Owen, R. Meier, *Science* **278**, 90 (1997).
8. E. Anders and N. Grevesse, *Geochim. Cosmochim. Acta* **53**, 197 (1989).
9. N. Biver *et al.*, *Bull. Am. Astron. Soc.* **29**, 1047 (1997). See also discussion in (1).
10. J. Crovisier, *Astron. Astrophys. Suppl. Ser.* **68**, 223 (1987).
11. Transition SO_2 $13_{2,12}-12_{1,11}$ at 345.3385391 GHz, if present, is to a large extent blended by the H^{13}CN 4–3 line [D. Bockelée-Morvan *et al.*, *Bull. Am. Astron. Soc.* **29**, 1047 (1997)]. The solution based on the hyperfine components of HCN 4–3 does not depend on the H^{13}CN line and shows that a potential SO_2 contamination is not detectable within the error bars.
12. At the time of the observations, the comet was passing in front of a Taurus molecular cloud, and we were careful to exclude the possibility of contamination by background sources. We took extensive measurements with and without the comet in the foreground. The day before the DCN measurement, the comet traversed L1497, a strong CO source with a bipolar velocity field (28). We could identify a double peak from the cloud in the wing of the cometary CO 3–2 line, blueshifted by about 2 km s^{-1} in the observer's frame of reference. No such wing extensions were seen in the cometary HCN 4–3 line. On the next day, when we recorded the DCN 5–4 spectrum, the CO line from the cloud was redshifted by ~ 3 to 4 km s^{-1} , consistent with low-resolution CO velocity maps of that area (28). In control measurements without the comet, we recovered all CO lines attributed to the cloud and demonstrated that an HCN 4–3 line (or any line other than CO lines) from the background sources was not detectable down to the 1% level relative to the cometary line at any of the positions of the comet. Summarizing, we exclude a contamination by emissions from the Taurus clouds for the following reasons: (i) Potential DCN lines from the cloud were either blueshifted or redshifted relative to the cometary line. (ii) For none of the positions in the cloud could we detect the HCN 4–3 or any line other than CO. (iii) On the basis of the Jet Propulsion Laboratory line atlas (29), there exists no line that—in the velocity frame of the cloud—may have serendipitously interfered with the cometary DCN position. (iv) Even if there were such a line, the observed FWHM still suggests a cometary origin because lines from the cloud are about half as wide. We were pointing 2° northwest of the deuterium-rich clumps TMC1 and TMC2.
13. D. Gautier and P. Morel, *Astron. Astrophys.* **323**, L9 (1997); J. Geiss, in *Origin and Evolution of the Elements*, N. Prantzos, E. Vangioni-Flam, M. Cassé, Eds. (Cambridge Univ. Press, Cambridge, 1993), pp. 89–106; H. Niemann *et al.*, *Science* **272**, 846 (1996).
14. C. Lecluse and F. Robert, *Geochim. Cosmochim. Acta* **58**, 2927 (1994).
15. B. Fegley Jr. and R. G. Prinn, in *The Formation and Evolution of Planetary Systems*, H. A. Weaver and L. Danly, Eds. (Cambridge Univ. Press, Cambridge, 1989), pp. 171–211.
16. A. Woollin, in *Astrochemistry*, M. S. Vardya and S. P. Tarafdar, Eds. (IAU Symposium 120, Reidel, Dordrecht, Netherlands, 1987), pp. 311–319; A. P. Jones and D. A. Williams, *Mon. Not. R. Astron. Soc.* **209**, 955 (1984).
17. T. J. Millar, A. Bennett, E. Herbst, *Astrophys. J.* **340**, 906 (1989).
18. P. D. Brown and T. J. Millar, *Mon. Not. R. Astron. Soc.* **237**, 661 (1989); T. Jacq *et al.*, *Astron. Astrophys.* **228**, 447 (1990).
19. J. M. Greenberg, in *Comets and the Origin of Life*, C. Ponnamparuma, Ed. (Reidel, Dordrecht, Netherlands, 1981), pp. 111–127.
20. A. P. Boss, G. E. Morfill, W. M. Tschamuter, in *Origin and Evolution of Planetary and Satellite Atmospheres*, S. K. Atreya, J. B. Pollack, M. S. Matthews, Eds. (Univ. of Arizona Press, Tucson, 1989), pp. 35–77; B. Dubrulle, *Icarus* **106**, 59 (1993).
21. J. I. Lunine, S. Engel, B. Rizk, M. Horanyi, *Icarus* **94**, 333 (1991).
22. This picture is consistent with the average formation temperature of 50 K for Oort cloud comets deduced from laboratory studies of noble gas trapping in ice [T. Owen and A. Bar-Nun, in *Conference Proceedings No. 341*, K. Farley, Ed. (American Institute of Physics, New York, 1995), pp. 123–138].
23. T. C. Owen and A. Bar-Nun, *Icarus* **116**, 215 (1995).
24. V. A. Krasnopolsky *et al.*, *Science* **277**, 1488 (1997); see also V. A. Krasnopolsky *et al.*, *IAU Circ.* 6625 (1997).

25. D. Gautier, B. J. Smith, T. Owen, I. de Pater, S. K. Atreya, in *Neptune and Triton*, D. P. Cruikshank, Ed. (Univ. of Arizona Press, Tucson, 1995), pp. 547–612.
26. W. M. Irvine and R. F. Knacke, in *Origin and Evolution of Planetary and Satellite Atmospheres*, S. K. Atreya, J. B. Pollack, M. S. Matthews, Eds. (Univ. of Arizona Press, Tucson, 1989), pp. 3–34.
27. R. Meier, D. Wellnitz, S. J. Kim, M. F. A'Hearn, in preparation.
28. H. Ungerechts and P. Thaddeus, *Astrophys. J. Suppl. Ser.* **63**, 645 (1987).
29. R. L. Pointner and H. M. Pickett, *Appl. Opt.* **24**, 2235 (1985).
30. K. Kim and W. T. King, *J. Chem. Phys.* **71**, 1967 (1979).
31. D. R. Bates and E. Herbst, in *Rate Coefficients in Astrochemistry*, T. J. Millar and D. A. Williams, Eds. (Kluwer Academic, Dordrecht, Netherlands, 1988), pp. 41–48. The predictions of D/H in H₂O may be changed by new experimental results on the dissociative electron recombination of H₃O⁺ and proton transfer to and from H₂O [T. L. Williams, N. G. Adams, L. M. Babcock, C. R. Herd, M. Geoghegan, *Mon. Not. R. Astron. Soc.* **282**, 413 (1996)].
32. We thank the operators of the JCMT for their assistance, B. Marsden and D. Tholen for help with the ephemerides, and P. Eberhardt for valuable comments on the manuscript. Supported by NASA grants NAEW 2650 and NAEW 2631. D.C.J. acknowledges support from NSF grant AST96-15603. The JCMT is operated by the Joint Astronomy Centre on behalf of the Particle Physics and Astronomy Research Council of the United Kingdom, the Netherlands Organisation for Scientific Research, and the National Research Council of Canada.

10 November 1997; accepted 2 February 1998

High-Selectivity, High-Flux Silica Membranes for Gas Separation

Renate M. de Vos and Henk Verweij

Process improvements in silica membrane fabrication, especially the use of clean-room techniques, resulted in silica membranes without detectable mesoscopic defects, resulting in significantly improved transport properties. Supported membranes calcined at 400°C were 30 nanometers in thickness, showed a H₂ permeance at 200°C of 2×10^{-6} moles per square meter per second per Pascal ($\text{mol m}^{-2} \text{s}^{-1} \text{Pa}^{-1}$), and had a CH₄ permeance more than 500 times smaller. Molecules larger than CH₄ were completely blocked. Silica membranes calcined at 600°C showed no detectable CH₄ flux, with a H₂ permeance of 5×10^{-7} ($\text{mol m}^{-2} \text{s}^{-1} \text{Pa}^{-1}$) at 200°C. These results signify an important step toward the industrial application of these membranes such as purification of H₂ and natural gas as well as the selective removal of CO₂.

The ability of amorphous microporous silica membranes with pore diameters (\varnothing) < 2 nm to pass small molecules while blocking larger ones has been known for years (1). State-of-the-art microporous silica membranes consist of a thin silica layer on top of a supported mesoporous (2 nm < \varnothing < 50 nm) γ -Al₂O₃ membrane, which provides mechanical strength. The key problem limiting industrial application of silica membranes is the poor reproducibility of the fabrication process, which results in large fluctuations in performance and often poor separation properties. Improving the membrane properties by lowering the defect size and density is currently one of the greatest challenges in inorganic membrane preparation.

Coherent and strong porous α -Al₂O₃ membrane supports were made from granulated alumina powder (2). The supports were uniaxially pressed at 10⁵ kPa to shape the disk, followed by isostatic pressing at 4000 kPa to achieve a higher and more uniform "green" density. They were then sintered at 1250°C to a final porosity of 40% with an average $\varnothing = 160$ nm. Membranes of γ -Al₂O₃ with $\varnothing = 2.5$ nm and a thickness of ~ 4 μm were prepared by dip-coating the supports in a boehmite sol followed by drying and calcining at 600°C (3). Dip-coating was performed by moving one side of the support

horizontally through the liquid surface of the sol solution for a few seconds. The whole process of dipping, drying, and calcining was repeated once, to repair any defects in the first γ -alumina layer. These defects could be caused by particle contamination, aggregates, microscopic air bubbles in the sol, and irregularities in the α -Al₂O₃ support surface. The γ -Al₂O₃ membranes, in turn, were used as a substrate for microporous silica membranes, prepared by dip-coating twice in a polymeric silica sol, followed by drying and calcining at 400° or 600°C (referred to as Si400 and Si600 membranes). The silica sol was prepared by acid-catalyzed hydrolysis and condensation of tetraethylorthosilicate (TEOS) (4) in ethanol as follows. A mixture of acid and water was carefully added to a mixture of TEOS and ethanol under vigor-

ous stirring. During the addition of the acid-water mixture, the TEOS-ethanol mixture was placed in an ice bath to avoid premature (partial) hydrolysis. After the addition was complete, the reaction mixture was refluxed for exactly 3 hours at 60°C in a water bath under continuous stirring. The reaction mixture had a final molar TEOS:ethanol:water:acid ratio (based on unreacted components) of 1:3.8:6.4:0.085 (5). All processing steps were well controlled, all liquids were filtered with a 0.5- μm filter, and nanoscale-particle processing was done in a clean room with class 1000 conditions. The dipping process was carried out in a flow cupboard in a clean air stream (class 10 conditions).

Well-controlled processing of every membrane fabrication step, clean process liquids, and the use of a clean room were important in membrane preparation. If the membrane preparation was done with extreme care but was not performed in a clean room, large defects and, hence, nonreproducible membranes were essentially inevitable. One defect with $\varnothing > 100$ nm per square centimeter of membrane surface led to substantial deterioration of all selectivities, especially those involving CH₄ and CO₂. The use of a clean room reduced the average concentration of particles of <0.5 μm in our normal laboratory air from 18 million per cubic meter to less than 100 m⁻³ in the flow cupboard where the membranes are prepared. Without clean-room conditions, the number of defects caused by particles from the air was estimated to be at least five defects of $\varnothing \approx 0.5$ μm per square centimeter of membrane surface. This num-

Table 1. Permselectivity (F_α) calculated from observed single-component permeances and selectivities (α) for 50/50 (V/V) gas mixtures for Si400 and Si600 at $\Delta P = 1$ bar and a mean pressure of 1.5 bar.

Mixture	Si400				Si600		
	100°C		200°C		100°C	200°C	300°C
	F_α	α	F_α	α	F_α	F_α	F_α
H ₂ /CO ₂	4.0	3.9	7.5	6.8	36	71	98
H ₂ /N ₂	61		64		>80	>135	>170
H ₂ /CH ₄	770	533	561	321	>2500	>4000	>5000
CO ₂ /CH ₄	194	118	75		>130	>100	>80
O ₂ /N ₂	3.9		3.3		>3	>6	>7

Laboratory for Inorganic Materials Science, Faculty of Chemical Technology, University of Twente, Post Office Box 217, 7500 AE Enschede, Netherlands.